ITUJournal
Future and evolving technologies

ITU Journal on Future and Evolving Technologies, Volume 6, Issue 1, March 2025

ARTICLE

Enhanced spectrum sensing for AI-enabled cognitive radio IoT with noise uncertainty

Md. Sipon Miah (Senior member, IEEE)[1,2,3], Michael Schukat[4], Enda Barrett[4], Maximo Morales Cespedes[2], Ana Garcia Armada[2]

[1] Department of Information and Communication Technology, Islamic University, Kushtia-7003, Bangladesh., [2] Department of Signal Theory and Communications, University Carlos III of Madrid, Leganes, Madrid, 28911, Spain, [3] Machine Learning-aided Wireless Communications (MLWC) Research Laboratory, Islamic University, Kushtia-7003, Bangladesh, [4] Department of Information Technology, University of Galway, Galway H91 TK33, Ireland.

Corresponding author: Md. Sipon Miah (Senior member, IEEE), sipon@ict.iu.ac.bd, mmiah@ing.uc3m.es

Spectrum sensing plays a major role in Cognitive Radio-based Internet of Things (CR-IoT) for identifying spectrum holes. However, a cooperative CR-IoT approach does not obtain sufficient sensing gain and sum-rate when using the conventional Energy Detection (ED) in an Noise Uncertainty (NU) environment, which may be aggravated under deep fading. To mitigate this problem, we propose an enhanced spectrum sensing technique and sum-rate calculation for Artificial Intelligence (AI)-enabled CR-IoT using the enhanced Kullback–Leibler Divergence (KLD). After a sensing phase, each CR-IoT user performs an enhanced KLD technique using local statistics, which allows us to reduce the required number of samples for reliable sensing. Then, each CR-IoT user sends its local decision to an AI-enabled Coordination Centre (AI-CC) that obtains a decision managing the channel fading state of the CR-IoT users. Finally, this decision is sent to an Fusion Centre (FC) that makes a global decision. The results obtained through simulations show that the proposed enhanced KLD technique achieves detection performance (86%) in comparison with conventional ED technique (69%) and KLD technique (97%) for an NU factor (ρ = 1.03), number samples (N_s = 30) and channel fading conditions.

Keywords: Artificial intelligence-enabled coordination, cognitive radio, energy consumption, global error probability, network lifetime, noise uncertainty, Internet of things, Kullback-Leibler divergence

1. INTRODUCTION

Internet of Things (IoT), based on continuous data sharing between sensor nodes that automatically enter and leave a network, is considered to be one of the most revolutionary communication technologies [1]. In this sense, the IoT concept has two fundamental characteristics, self-adaptation and self-organization. However, future IoT networks face challenges such as spectrum shortage, high deployment cost, and high energy consumption, which involve a large number of devices and a more flexible management of the available bandwidth [2].

Cognitive Radio (CR) is a promising wireless communication technology that improves spectrum efficiency by flexibly managing spectrum slots [3]. In a Cognitive Radio IoT (CR-IoT) network, each CR-IoT user occupies the spectrum only when it is empty. CR-IoT users adopt a spectrum sensing approach, i.e. a channel discovery mechanism is carried out to select the channels that are most suitable for secondary access. Following this approach, each CR-IoT user accesses licensed spectrum opportunistically without causing any harmful interference with the Primary User (PU). When the PU returns, the secondary user vacates the spectrum immediately. Therefore, the CR technology allows secondary IoT systems to exploit the available underused spectrum opportunistically by adjusting their transmission modes, while guaranteeing there is no interference with primary IoT systems [4].

Spectrum sensing techniques can be classified into several categories, such as non-coherent detection, coherent detection, non-cooperative detection, and cooperative detection [5]. In a non-coherent detection, spectrum sensing is performed without any requirement for prior knowledge of the PU's signal. In contrast, for coherent detection, prior knowledge of the PU's signal is required. Another criterion of classification is the cooperation level among CR-IoT users. In non-cooperative detection, the detection of the PU's signal is based on local observations of a single CR-IoT user. In this case, the spectrum sensing performance is compromised because of multipath fading and shadowing effects [6]. In cooperative detection, each individual CR-IoT user performs local sensing independently, and then forwards the sensing result to the Fusion Centre (FC) through a reporting channel. With these reported local results the FC makes a global decision based on a fusion rule [7]. It is worth noticing that this cooperative approach can solve the problem of local sensing [8].

Based on classification, several spectrum sensing techniques, such as Energy Detection (ED), matched filter detection, and cyclostationary feature detection, have been proposed subject to a variety of fading channels [9, 10, 11, 12]. Among the aforementioned spectrum sensing techniques, the ED technique has the advantages of low complexity and cost effectiveness. Thus, it is especially suitable for performing spectrum sensing without any prior information about the PU's signal pattern. Moreover, the ED technique is a full blind process that does not require information about wireless channel gains or other parameters about the PU's signal. However, the exact information of the noise power at the receiver side, i.e. the sensing side of the CR-IoT user is essential for an accurate detection. In an Noise Uncertainty (NU) environment [13], the performance degradation of the ED technique is inevitable. Even for cooperative detection, the performance gain obtained is limited [14]. For the low-power operation of the CR-IoT users, the sensing time should be minimized as much as possible. As a consequence, subject to short sensing intervals, the conventional ED technique is not suitable for detection of the PU's signal.

During the last few years, several pieces research works have been focused on solving the aforementioned issues assuming cooperative spectrum sensing in CR-IoT networks. In [15], the CR-IoT users perform their local sensing, report soft decisions to the FC, and store this information in a local database. The FC determines the Kullback-Leibler Divergence (KLD) score against each CR-IoT user, and sends this information to all CR-IoT users. In general, every user attempts to send the mean of the previous energy reports to the FC based on its current observation. In [16], the authors propose the use of KLD to evaluate the dissimilarity in the probability distribution functions under the hypotheses presence and the absence of the PU's signal. In [17], each CR-IoT user provides information about their local spectrum observations of the licensed spectrum to an FC that collects the local sensing results and makes its global decision. Before doing this, the FC assigns weights, which are proportional to the reliability of the local spectrum sensing information, for local sensing of the CR-IoT users. The approach of [17] is analyzed considering the presence of fading channels without considering an NU environment. However, the spectrum sensing performance based on the conventional ED or KLD techniques does not exclude the deep fading CR-IoT users at the FC subject to an NU environment. To the authors' best knowledge, the sensing performance (sum-rate, energy consumption, longer network lifetime, global error probability and cooperative overheads), taking into account the effects of the NU while managing the deep fading CR-IoT users, automatically based on the concept of the artificial intelligence coordinator centre, have not been previously evaluated for a CR-IoT network.

1.1 Contributions

The main contributions of this paper can be summarized as follows:

- We proposed an enhanced spectrum sensing for an Artificial Intelligence (AI)-enabled CR-IoT in NU environments. Each CR-IoT user achieves an enhanced sensing performance, even with a small number of samples, using the KLD technique. Moreover, we provide an analytical estimation of the enhanced sensing performance of the AI-enabled Coordinator Centres (AI-CCs) and an FC using the soft fusion rule. For this approach, the AI-CC computes the measurement of the dissimilarity between two Gaussian distributions under two hypotheses, which excludes the deep fading CR-IoT users; here each CR-IoT user receives fluctuation of SNR values.
- Based on the enhanced sensing performance, the sum-rate of the primary and secondary IoT networks, i.e., the cognitive network, is analyzed compared to the conventional ED technique with (and without) an NU environment, the conventional KLD technique without an NU environment, and the proposed enhanced KLD technique with an NU environment using the soft fusion rule subject to different fading channel conditions.
- In such a way, the energy efficiency, the network lifetime, the global error probability, and the reporting overheads are also analyzed for the considered sensing techniques.

1.2 Organization

The remainder of this paper is organized as follows. In Section 2, the IoT system model is described. The conventional ED technique in an NU environment is discussed in Section 3. Section 4 includes the proposed scheme for future IoT deployments, wherein the analyses of the spectrum sensing, the sum-rate, energy consumption, the network lifetime, the global error probability and the reporting overhead are performed based on the proposed enhanced KLD technique under a variety of fading channels in an NU environment. The numerical and simulation results and their discussion are presented in Section 5. Finally, concluding remarks are provided in Section 6.

2. SYSTEM MODEL

The proposed IoT system model comprises both a primary IoT system and secondary IoT system links as shown in Fig. 1. The secondary IoT network shares the licensed spectrum band with the primary IoT network by opportunistically accessing the underutilized spectrum when the primary IoT user is inactive. In this section, the primary IoT network, and the secondary IoT network, the so-called an AI-enabled CR-IoT network, are presented.

2.1 The primary IoT network

The primary IoT network consists of the primary IoT transmitter and receiver denoted by $\mathrm{PU_{tx}}$ and $\mathrm{PU_{rx}}$, respectively. The operation of the primary IoT user (PU) follows a Time Division Multiple Access (TDMA) scheme. Since PU activity is closely related to the performance of CR-IoT networks, the estimation of this activity plays a major role in spectrum sensing. The PU activity is modelled by two state Markov chain [18]. Thus, there are two possible states; **off(0)** and **on(1)**. In **off(0)** state, the licensed channel is free from the PU while in state **on(1)**, the licensed channel is currently occupied by the PU. Without loss of generality, we assume that the duration of the P_0 = **off(0)** and P_1 =**on(1)** states are represented by the random variables Θ_1 and Θ_2, which follow an exponential distribution with mean duration R and S, respectively. Moreover, these distributions are independent between them. At any time, the probabilities that the PU is in either the P_0 or P_1state are given by $P_0 = R/(R+S)$, and $P_1 = S/(R+S)$, respectively.

2.2 The AI-enabled CR-IoT network

The AI-enabled CR-IoT network consists of M CR-IoT users, $M_{\mathrm{AI-CC}}$ AI-CCs and an FC. The set of CR-IoT users belonging to the j^{th} AI-CC, $j = 1, 2, \cdots, M_{\mathrm{AI-CC}}$, is

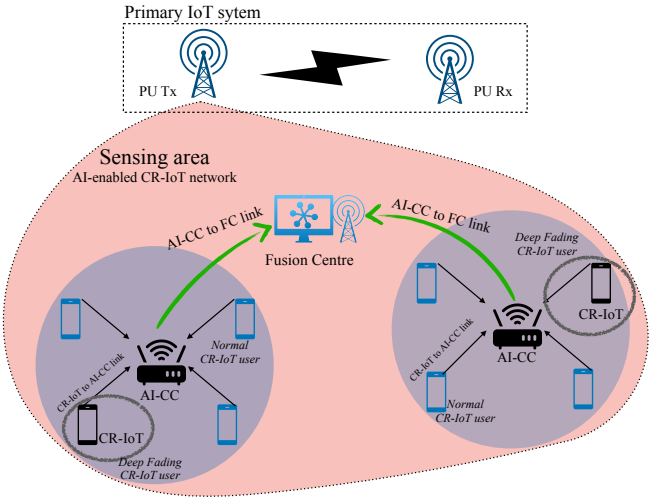

Figure 1 – The proposed IoT system model with a primary IoT network and an AI-enabled CR-IoT network including some AI-CCs and an FC.

denoted by M_{CC}. A representation of this network is shown in Fig. 1, the i^{th} CR-IoT user reports their local sensing information of the PU channel to the j^{th} AI-CC. Then, the j^{th} AI-CC collects the local sensing information from the i^{th} CR-IoT user, which obtains local decision statistics. After that, the j^{th} AI-CC forwards their local decision statistics to the FC. Then, the FC collects the local decision statistics from all AI-CCs and generates a global decision to show the actual status of the PU spectrum.

For a binary hypothesis testing problem, we define the two hypotheses H_k, $k = \{0, 1\}$, representing the absence and presence of the PU's signal as follows:

$$\begin{cases} H_{k=0}; & \text{if the PU's signal is absent,} \\ H_{k=1}; & \text{if the PU's signal is present,} \end{cases} \tag{1}$$

Depending on the state of the PU, the received signal of the i^{th} CR-IoT user in the j^{th} AI-CC at the l^{th} sample, $l = \{1, 2, \cdots, N_s\}$, under the two hypotheses is given by [8]

$$y_{i,j}(l) = \begin{cases} n_{i,j}(l); & H_{k=0} \\ h_{i.j}(l)\, x(l) + n_{i,j}(l); & H_{k=1} \end{cases} \tag{2}$$

where $h_{i,j}(l)$ is the channel gain between the i^{th} CR-IoT user at the j^{th} AI-CC and the primary transmitter for $i = \{1, 2, \cdots, M\}$, $j = \{1, 2, \cdots, M_{\mathrm{CC}}\}$, $x(l)$ is a signal transmitted from the PU, which is modulated by a Binary Phase Shift Keying (BPSK) with a power equal to p_x^2, and $n_{i,j}(l)$ is a circularly symmetric complex Gaussian noise of the i^{th} CR-IoT user at the j^{th} AI-CC with a variance of $\sigma^2_{n,i,j}$ [19]. Moreover, it is assumed that the channel remains constant during each sensing phase.

3. CONVENTIONAL ENERGY DETECTION TECHNIQUE

The ED process performed by the CR-IoT users is described in Fig. 2. First, a band-pass filter is applied to the received signal to select the appropriate signal bandwidth, and the output of this filter is then transformed by an Analogue-to-Digital Converter (ADC). Here, the analogue signal is sampled to obtain a discrete signal, which is individually averaged and squared for the conventional ED technique to estimate its own received signal energy [20]. The measured energy of the i^{th} CR-IoT user at the j^{th} AI-CC is expressed as follows,

$$e_{i,j} = \sum_{l=0}^{N_s-1} \left| y_{i,j}(l) \right|^2, \tag{3}$$

where N_s denotes the total number of signal samples used for the sensing with a sampling frequency of f_s. Therefore, the duration of the sensing time slot is given by $\tau_s = \frac{N_s}{f_s}$.

Figure 2 – Block diagram of the conventional ED technique [20].

3.1 Sensing performance

Spectrum sensing is the basic and essential mechanism of CR to find the unused spectrum holes that are allocated for the licensed PUs. In this paper, we derive a mathematical model that shows the influence of the NU on the ED technique's performance [13]. It can be represented by an NU factor denoted by $\rho \geq 1$. For an NU factor $\rho = 1$ there is no variation in the intensity of the noise. Thus, the conventional ED technique can be considered in this case. On the other hand, if $\rho > 1$ means that the ED is subject to an NU, i.e., higher ρ values mean higher variation in the intensity of the noise [13, 21].

Proposition 1: Based on the Central Limit Theorem (CLT), the distribution of the local decision statistics, $e_{i,j}$ of the i^{th} CR IoT user at the j^{th} AI-CC under both hypotheses with an NU environment [22] can be expressed as

$$e_{i,j} \sim \begin{cases} \aleph\left(\mu_{0,i,j}(H_0), \sigma^2_{0,i,j}(H_0)\right) \\ \aleph\left(\mu_{1,i,j}(H_1), \sigma^2_{1,i,j}(H_1)\right) \end{cases} \tag{4}$$

where $\mu_{0,i,j}(H_0) = \rho N_s \sigma^2_{n,i,j}$, $\sigma^2_{0,i,j}(H_0) = \rho N_s \sigma^4_{n,i,j}$, $\mu_{1,i,j}(H_1) = \frac{N_s}{\rho}\left(1 + |h_{i,j}|^2 \gamma_{i,j}\right)\sigma^2_{n,i,j}$, $\sigma^2_{1,i,j}(H_1) = \frac{N_s}{\rho}\left(1 + 2|h_{i,j}|^2 \gamma_{i,j}\right)\sigma^4_{n,i,j}$ and $\gamma_{i,j}$ is the SNR that is defined as $\gamma_{i,j} = \frac{p_x^2}{\sigma^2_{n,i,j}}$. Moreover, ρ is a NU factor.

Proof. Please see Appendix A. □

The probability of a false alarm, $p_{f,j}$, is the probability that the AI-CC j incorrectly declares that the PU exists although the PU is actually absent, while the probability of detection, $p_{d,j}$, denotes the probability that the AI-CC j correctly declares that the PU is present. Based on *(4)*, $p_{f,j}$ and $p_{d,j}$ can be calculated comparing $e_{i,j}$ with a predefined threshold, $\lambda^{\text{ED}}_{i,j}$ [23]. That is,

$$\begin{aligned} p_{f,j} &= \Pr\left[e_{i,j} \geq \lambda^{\text{ED}}_{i,j} | H_{k=0}\right] \\ &= Q\left(\frac{\lambda^{\text{ED}}_{i,j} - \mu_{0,i,j}(H_0)}{\sigma_{0,i,j}(H_0)}\right) = Q\left(\frac{\lambda^{\text{ED}}_{i,j}}{\sqrt{\rho N_s}\sigma^2_{n,i,j}} - \sqrt{\rho N_s}\right) \end{aligned} \tag{5}$$

$$\begin{aligned} p_{d,j} &= \Pr\left[e_{i,j} \geq \lambda^{\text{ED}}_{i,j} | H_{k=1}\right] = Q\left(\frac{\lambda^{\text{ED}}_{i,j} - \mu_{1,i,j}(H_1)}{\sigma_{1,i,j}(H_1)}\right) \\ &= Q\left(\frac{\lambda^{\text{ED}}_{i,j}}{\sigma^2_{n,i,j}\sqrt{\frac{N_s}{\rho}\Delta h}} - \frac{\sqrt{\frac{N_s}{\rho}}(1 + |h_{i,j}|^2\gamma_{i,j})}{\sqrt{\Delta h}}\right), \end{aligned} \tag{6}$$

where $Q(x)$ denotes a Gaussian tail function defined as $Q(x) = \frac{1}{\sqrt{2\pi}}\int_x^\infty e^{-\left(\frac{\zeta^2}{2}\right)} d\zeta$ and $\Delta h = (1 + 2|h_{i,j}|^2\gamma_{i,j})$

Therefore, comparing the test statistic, $e_{i,j}$ with a predefined threshold, $\lambda^{\text{ED}}_{i,j}$, we can determine whether there is a signal or not. That is, if $e_{i,j} \geq \lambda^{\text{ED}}_{i,j} | H_{k=1}$, the PU signal is present; otherwise, the PU signal is not present.

Proposition 2: In a system subject to NU given by a factor, ρ, the decision threshold, $\lambda^{\text{ED}}_{i,j}$ at the i^{th} CR-IoT user of the j^{th} AI-CC for a determined probability of false alarm and detection, can be expressed, respectively, as

$$\lambda^{\text{ED}}_{i,j}\left(p_f\right) = \sqrt{\rho N_s}\sigma^2_{n,i,j}\left(Q^{-1}\left(p_{f,j}\right) + \sqrt{\rho N_s}\sigma^2_{n,i,j}\right) \tag{7}$$

and

$$\lambda^{\text{ED}}_{i,j}(p_d) = \frac{1}{\sqrt{\frac{N_s}{\rho}}K\sigma^2_{n,i,j}}\left(Q^{-1}\left(p_{d,j}\right) + \sqrt{\frac{N_s}{\rho}}K\right), \tag{8}$$

where $K = \sqrt{(1 + 2|h_{i,j}|^2\gamma_{i,j})}$, $p_{d,j} \in p_d$, and $p_{f,j} \in p_f$. Notice that p_d, and p_f are constant for the sake of simplicity.

Proof. Please see Appendix B. □

Proposition 3: In an NU environment based on ED, the minimal number of samples for a perfect detection of the

PU signal depends on the target probability of detection, false alarm and an NU factor. It can be expressed as

$$N_s^{min} = \frac{\left[\sqrt{\rho}KQ^{-1}\left(p_{d,j}^*\right) - \rho^{3/2}Q^{-1}\left(p_{f,j}^*\right)\right]^2}{\left[\rho^2 - K^2\right]^2}, \quad (9)$$

where, N_s^{min} denotes the minimal number of samples, p_d^* denotes the target probability of detection, and p_f^* denotes the target probability of false alarm.

Proof. Please see Appendix C. □

At the FC, all the local decision statistics of the AI-CCs are combined with the local results to obtain a global decision about the PU occupancy of the spectrum. The sensing performance of the global decision is given by

$$p_{f,\mathrm{FC}}^{\mathrm{ED}} = \begin{cases} 1, & \text{if } \sum_{j=1}^{M_{\mathrm{CC}}} p_{f,j} < \beta_{\mathrm{ED}}, \\ 0, & \text{otherwise}, \end{cases} \quad (10)$$

and

$$p_{d,\mathrm{FC}}^{\mathrm{ED}} = \begin{cases} 1, & \text{if } \sum_{j=1}^{M_{\mathrm{CC}}} p_{d,j} \geq \beta_{\mathrm{ED}}, \\ 0, & \text{otherwise}, \end{cases} \quad (11)$$

where β_{ED} denotes the global decision threshold at the FC where the value of β_{ED} depends on the number of CR-IoT users participate in sensing.

3.2 Sum-rate analysis

Based on the global sensing performance, the sum-rate, R^{ED} can be evaluated as

$$R^{\mathrm{ED}} = P_1 p_{d,\mathrm{FC}}^{\mathrm{ED}} R_{\mathrm{PU}} + P_0\left(1 - p_{f,\mathrm{FC}}^{\mathrm{ED}}\right) R_{\mathrm{CR-IoT},i,j}, \quad (12)$$

where R_{PU} denotes the channel achievable rate of the PU link, and $R_{\mathrm{CR-IoT},i,j}$ denotes the achievable rate of the CR-IoT link.

3.3 Energy consumption analysis

The average energy consumption of the conventional ED technique with an NU environment can be measured [24] as

$$E_{avg}^{\mathrm{ED}} = E_s\tau_s + E_tT_t\left[\left(1 - p_{f,\mathrm{FC}}^{\mathrm{ED}}\right)P_0 + \left(p_{d,\mathrm{FC}}^{\mathrm{ED}}\right)P_1\right], \quad (13)$$

where T_t denotes the transmission time, E_s denotes the energy consumed for the sensing time slot, and E_t denotes the energy consumed for the data transmission.

3.4 Network lifetime analysis

In the conventional ED technique with an NU environment [24], we can calculate the expected network lifetime i.e., the maximum number of time slots that the CR-IoT network can be powered by the battery as $\eta^{\mathrm{ED}} = \frac{E_c}{E_{avg}^{\mathrm{ED}}}$ where E_c is the capacity of batteries in J.

3.5 Global error probability

The global error probability, p_e^{ED} at the FC can be estimated with an NU factor [25, 24, 26], which is given as

$$p_e^{\mathrm{ED}} = P_1\left(1 - p_{d,\mathrm{FC}}^{\mathrm{ED}}\right) + P_0 p_{f,\mathrm{FC}}^{\mathrm{ED}}, \quad (14)$$

where p_e is the global error probability.

3.6 Total time analysis

We can calculate the total time required by the conventional ED technique with an NU environment as

$$\tau_t^{\mathrm{ED}} = \tau_{dp} + \tau_s + \sum_{i=1}^{M}\tau_{r,i} = \tau_{dp} + \tau_s + M\tau_r, \quad (15)$$

where τ_t^{ED} is the total sensing time in the conventional ED technique τ_r is the reporting time of the each CR-IoT user which is a fixed, and τ_{dp} is the decision processing time which is a constant. Therefore, the total time, τ_t^{ED}, is only dependent on the number of CR-IoT users M. Notice that, as M increases, the cooperative sensing performance of the conventional ED technique for non-grouping is enhanced but the overhead for cooperation increases.

4. PROPOSED ENHANCED KLD TECHNIQUE FOR AN AI-ENABLED CR-IOT NETWORK

In this section, conventional spectrum sensing based on KLD and the proposed enhancements are described. The sum-rate, energy consumption, network lifetime, global error probability, and total time analysis are discussed.

4.1 Spectrum sensing analysis

4.1.1 KLD technique without an NU environment

The conventional KLD technique is based on measuring the asymmetry of two probability density functions (pdf) [17, 15]. Specifically, the KLD value for two generic

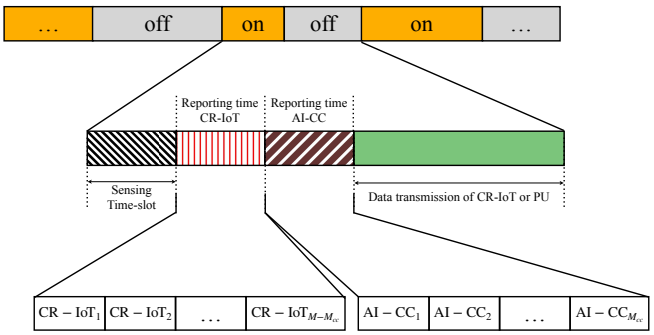

Figure 3 – Frame structure of a time slot for reporting sensing information and packet transmission.

pdfs $g(y)$ and $f(y)$ is given by

$$\mathrm{KLD}\left(g\|f\right) = \int g(y) \times \log\left(\frac{g(y)}{f(y)}\right) dy, \tag{16}$$

where $g(y)$ is pdf related with the sensed information when the PU is present and $f(y)$ is pdf related with the sensed information when the PU is absent.

Thus, the KLD(j) value at the j^{th} AI-CC for the conventional KLD technique without considering an NU environment, i.e., assuming $\rho = 1$ based on the means $\left(\mu_{0,i,j}(c), \mu_{1,i,j}(c)\right)$, and variances $\left(\sigma^2_{0,i,j}(c), \sigma^2_{1,i,j}(c)\right)$ is

$$\mathrm{KLD}(j) = \mathrm{KLD}\left(\mu_{0,i,j}(c), \mu_{1,i,j}(c), \sigma^2_{0,i,j}(c), \sigma^2_{1,i,j}(c)\right)$$
$$= \frac{1}{2}\left[\log\left(\frac{\sigma^2_{0,i,j}(c)}{\sigma^2_{1,i,j}(c)}\right) - 1 + \left(\frac{\sigma^2_{1,i,j}(c)}{\sigma^2_{0,i,j}(c)}\right) + \frac{\left(\mu_{1,i,j}(c) - \mu_{0,i,j}(c)\right)^2}{\sigma^2_{0,i,j}(c)}\right] \tag{17}$$

where $\mu_{0,i,j}(c) = N_s\sigma^2_{n,i,j}$, $\sigma^2_{0,i,j}(c) = N_s\sigma^4_{n,i,j}$, $\mu_{1,i,j}(c) = N_s\left(1 + |h_{i,j}|^2\gamma_{i,j}\right)\sigma^2_{n,i,j}$ and $\sigma^2_{1,i,j}(c) = N_s\left(1 + 2|h_{i,j}|^2\gamma_{i,j}\right)\sigma^4_{n,i,j}$ Here, c indicates the conventional KLD technique without considering an NU environment.

4.1.2 *The proposed enhanced KLD technique for NU environments*

Under the frame structure presented in Fig. 3, all the CR-IoT users sense the PU's channel during a sensing time slot, τ_s, using the KLD technique for an NU environment ($\rho \neq 1$) and they report to an FC using different reporting time slots due to a reduced channel overhead when the number of CR-IoT users increases in the proposed scheme. Based on the definition, the KLD technique computes the difference between two probability distributions in the same event space under two hypotheses $\mathcal{S}(H_0, H_1)$, where: (i) the larger the KLD value means the greater dissimilarity between two hypotheses, (H_0, H_1), and (ii) if the KLD value is zero it means there is no dissimilarity between the two hypotheses, (H_0, H_1). For this approach, the AI-CC computes the measurement of the dissimilarity between two Gaussian distributions under two hypotheses, which excludes the deep fading CR-IoT users due to the fact that the KLD value of hypothesis H_1 and H_0 decreases as the strength value of the deep fading effect increases. Therefore, the AI-CC makes the local decision statistics with high robustness, so that the KLD value between hypothesis H_1 and H_0 are as large as possible.

The KLD representation of the two Gaussian distributions of $e_{i,j}(H_1)$, and $e_{i,j}(H_0)$ in *(4)* with H_0, and H_1, respectively, is required to be evaluated. Therefore, the means are calculated under two hypotheses with the updated equations as

$$\mu_{k,i,j} = \tilde{\mu}_{k,i,j} + e_{i,j}(H_k), \tag{18}$$

where $\mu_{k,i,j}$ is the updated mean value for the i^{th} CR-IoT user at the j^{th} AI-CC for hypothesis $k = \{0, 1\}$. These values are updated with the previous mean values, i.e., $\tilde{\mu}_{0,i,j} = \rho N_s\sigma^2_{n,i,j}$ and $\tilde{\mu}_{1,i,j} = \rho N_s\sigma^4_{n,i,j}$. Moreover, $e_{i,j}$ is the received energy under the respective hypotheses. Similarly, the variances are updated based on the received energy, $e_{i,j}$,

$$\sigma^2_{k,i,j} = \tilde{\sigma}^2_{k,i,j} + [e_{i,j}(H_k) - \mu_{k,i,j}]^2, \tag{19}$$

where $\sigma^2_{k,i,j}$ is the updated variance value for the i^{th} CR-IoT user at the j^{th} AI-CC for hypothesis $k = \{0, 1\}$, which is updated with the previous variance values, i.e., $\tilde{\sigma}^2_{0,i,j} = \frac{N_s}{\rho}\left(1 + |h_{i,j}|^2\gamma_{i,j}\right)\sigma^2_{n,i,j}$ and $\tilde{\sigma}^2_{1,i,j} = \frac{N_s}{\rho}\left(1 + |h_{i,j}|^2\gamma_{i,j}\right)\sigma^4_{n,i,j}$, under the two possible hypotheses.

After updating the mean and variance information on behalf of all M_{CC} CR-IoT users at the j^{th} AI-CC, the particular CR-IoT user measures the difference in the mean and variance of the i^{th} CR-IoT user energy statistics from those of all other CR-IoT users. The average mean values are measured on behalf of all the M_{CC} CR-IoT users based on the new mean and variance values, which are given by *(18)* and *(19)*, respectively. Thus, the average means are

$$\bar{\mu}_{k,i,j} = \frac{\sum_{i=1}^{M_{\mathrm{CC}}} \mu_{k,i,j} - \mu_{k,i,j}}{(M_{\mathrm{CC}} - 1)}, \tag{20}$$

where $\bar{\mu}_{k,i,j}$ is the average mean value of the energy samples provided by all other users except the i^{th} CR-IoT user at the j^{th} AI-CC due to exclusions of the deep fading CR-IoT users under hypotheses $k = \{0, 1\}$. Furthermore, we can calculate the average variances as

$$\bar{\sigma}^2_{k,i,j} = \frac{\sum_{i=1}^{M_{\mathrm{CC}}} \sigma^2_{k,i,j} - \sigma^2_{k,i,j}}{(M_{\mathrm{CC}} - 1)}, \tag{21}$$

where $\bar{\sigma}^2_{k,i,j}$ are values of the energy samples provided by all other users while ignoring the variance of the i^{th} CR-IoT user under hypotheses $k = \{0, 1\}$. That is, these variances are obtained by excluding the i^{th} CR-IoT user.

From *(20)* and *(21)*, we obtain M_{CC} different statistics for the channel sensing with different combinations of CR-IoT users. Considering fading effects, some of the CR-IoT users could experience significantly deep fading. In this case, these CR-IoT users may report incorrect sensing results. To mitigate such a problem, we employ multiple decision statistics based on the various combinations of the CR-IoT users which exclude the deep fading CR-IoT users. Using this approach, we can prevent the occurrence of a global channel sensing error caused by a few users under deep fading channels. Thus, after calculating the means and variances, the j^{th} AI-CC obtains the local decision statistics based on the proposed enhanced KLD technique as

$$\begin{aligned}\overline{\mathrm{KLD}}(j) &= \overline{\mathrm{KLD}}\left(\bar{\mu}_{0,i,j}, \bar{\mu}_{1,i,j}, \bar{\sigma}^2_{0,i}, \bar{\sigma}^2_{1,i,j}\right) \\ &= \frac{1}{2} \times \left[\log\left(\frac{\bar{\sigma}^2_{0,i,j}}{\bar{\sigma}^2_{1,i,j}}\right) - 1 + \left(\frac{\bar{\sigma}^2_{1,i,j}}{\bar{\sigma}^2_{0,i,j}}\right) + \frac{\left(\bar{\mu}_{1,i,j} - \bar{\mu}_{0,i,j}\right)^2}{\bar{\sigma}^2_{0,i,j}}\right]\end{aligned} \tag{22}$$

Theorem 1: In an NU environment, the proposed enhanced $\overline{\mathrm{KLD}}(j)$ value at the j^{th} AI-CC is greater than the conventional KLD(j). Since the harmful deep fading CR-IoT user does not participate in the sensing as normal CR-IoT users, the enhanced sensing performance is given by

$$\overline{\mathrm{KLD}}(j) = \frac{1}{2}\left[\log\left(\frac{\sigma^2_{0,j}}{\sigma^2_{1,j}}\right)\right] + \mathrm{KLD}(j). \tag{23}$$

Proof. Please see Appendix D. □

Theorem 2: In the proposed enhanced KLD technique, the $\overline{\mathrm{KLD}}(j)$ value of hypothesis H_1 and H_0 at the j^{th} AI-CC is zero, i.e., it cannot distinguish between non-deep fading and deep fading CR-IoT users, if all CR-IoT users have the same SNR values $\left(\gamma = \sum \gamma_{i,j}\right)$. Then, the sensing performance at j^{th} AI-CC is severely degraded due to the harmful deep fading CR-IoT users participating in the sensing as normal CR-IoT users so that

$$\overline{\mathrm{KLD}}(j) = \overline{\mathrm{KLD}}\left(\bar{\mu}_{0,i,j}, \bar{\mu}_{1,i,j}, \bar{\sigma}^2_{0,i,j}, \bar{\sigma}^2_{1,i,j}\right) = 0. \tag{24}$$

Proof. Please see Appendix E. □

All the AI-CCs send their local decision statistics based on the proposed enhanced KLD technique to the FC. After that, the FC collects the local decision statistics information and makes a global decision. The sensing performance can be evaluated by $(p^{\overline{\mathrm{KLD}}}_{f,\mathrm{FC}}/p^{\overline{\mathrm{KLD}}}_{d,\mathrm{FC}})$ at the FC as

$$p^{\overline{\mathrm{KLD}}}_{f,\mathrm{FC}} = \begin{cases} 1, & \text{if } \sum_{j=1}^{M_{\mathrm{CC}}} \overline{\mathrm{KLD}}(j) < \beta_{\mathrm{KLD}} \\ 0, & \text{otherwise} \end{cases} \tag{25}$$

and

$$p^{\overline{\mathrm{KLD}}}_{d,\mathrm{FC}} = \begin{cases} 1, & \text{if } \sum_{j=1}^{M_{\mathrm{CC}}} \overline{\mathrm{KLD}}(j) \geq \beta_{\mathrm{KLD}} \\ 0, & \text{otherwise} \end{cases} \tag{26}$$

where β_{KLD} denotes the global decision threshold at the FC, here the value of β_{ED} depends on the number of CR-IoT users participate in sensing.

In the proposed enhanced KLD sensing technique, the probabilities of false alarm, and detection cannot be obtained analytically because the distribution of the KLD is not available. Therefore, numerical results are employed for the evaluation of the sensing performance.

4.2 Sum-rate analysis

Using the frame structure and sensing performance described above, the sum-rate can be determined considering some assumptions. First, let us consider that the CR-IoT transmitter follows a round-robin scheduling. Thus, in a non-false alarm event, the unlicensed CR-IoT user can access the primary spectrum with the probability $\left(1 - p^{\overline{\mathrm{KLD}}}_{f,\mathrm{FC}}\right)$, while in a detection event, the PU's transmission is not interfered with by the CR-IoT users. Therefore, the sum-rate of both the PU and the CR-IoT users is given by

$$R^{\overline{\mathrm{KLD}}} = P_1 p^{\overline{\mathrm{KLD}}}_{d,\mathrm{FC}} R_{\mathrm{PU}} + P_0\left(1 - p^{\overline{\mathrm{KLD}}}_{f,\mathrm{FC}}\right) R_{\mathrm{CR-IoT}}, \tag{27}$$

where R_{PU} is the achievable rate of the PU link, $R_{\mathrm{CR-IoT}}$ is the achievable rate of the CR-IoT link and P_0 & P_1 are the primary activity factors, which indicates the probability of the PU's transmission in a given frame. R_{PU} and $R_{\mathrm{CR-IoT}}$ are defined as

$$R_{\mathrm{PU}} = \log_2\left(1 + \mathrm{SNR}_{\mathrm{PU}}\right) \tag{28}$$

and

$$R_{\mathrm{CR-IoT}} = \frac{T - \tau_s}{T} \sum_{i=1}^{M} \log_2\left(1 + \mathrm{SNR}_{\mathrm{CR-IoT},i,j}\right), \tag{29}$$

where $\mathrm{SNR}_{\mathrm{PU}}$ and $\mathrm{SNR}_{\mathrm{CR-IoT},i}$ denote the SNR of the PU's link and the i^{th} CR-IoT link, respectively, and T denotes the total frame length.

4.3 Energy consumption analysis

The average energy consumption of the proposed enhanced KLD technique for an NU environment can be measured as

$$E^{\overline{\mathrm{KLD}}}_{\mathrm{avg}} = E_s\tau_s + E_t T_t\left(\left(1 - p^{\overline{\mathrm{KLD}}}_{f,\mathrm{FC}}\right)P_0 + \left(p^{\overline{\mathrm{KLD}}}_{d,\mathrm{FC}}\right)P_1\right), \tag{30}$$

where T_t is the transmission time, which is defined as $T_t = T - \tau_s - \tau_r - \tau_{dp}$, E_s is the energy consumed for the

sensing time slot, T is duration of the entire time slot, P_0 and P_1 denotes the probability of absence of the PU and the probability of presence of the PU, respectively, and E_t is the energy consumed for the data transmission.

4.4 Network lifetime analysis

The expected network lifetime of the proposed enhanced KLD technique is given by

$$\eta^{\overline{\text{KLD}}} = \frac{E_c}{E_{\text{avg}}^{\overline{\text{KLD}}}}, \tag{31}$$

where E_c is the capacity of battery in Jule.

4.5 Global error probability

The global error probability at the FC, denoted by p_e, is given by

$$p_e^{\overline{\text{KLD}}} = P_1\left(1 - p_{d,\text{FC}}^{\overline{\text{KLD}}}\right) + P_0 p_{f,\text{FC}}^{\overline{\text{KLD}}}. \tag{32}$$

4.6 Total time analysis

For proposed enhanced KLD technique, the total decision processing time, sensing time and reporting time, denoted by τ_t, which comprises the decision processing time, τ_{dp}, the sensing time, τ_s, and reporting time, τ_r, increases with the number of CR-IoT users.

Proposition 4: The total time required by the proposed enhanced KLD technique is

$$\tau_t^{\overline{\text{KLD}}} = \tau_{dp} + \tau_s + \left(\frac{M + M_{\text{NCC}}^2}{M_{\text{NCC}}}\right)\tau_r, \tag{33}$$

where τ_r is the reporting time for the CR IoT users. While the sensing time, τ_s, is shared by all CR-IoT users, the reporting time, τ_r, is not shared. Therefore, the total time, τ_t, depends on the number of the CR-IoT users at each AI-CC, which is denoted by M and the number of AI-CCs, M_{NCC}.

Proof. Please see Appendix F. □

Notice that as M increases, the cooperative sensing performance is enhanced but the overhead for cooperation decreases by the grouping in the proposed enhanced KLD technique. Therefore, we conclude that the overhead of the proposed enhanced KLD technique is less than the conventional ED and KLD techniques, i.e., $M_{\text{CC}} < M$.

In Algorithm 1, the entire process for obtaining the global decision at the FC is described where an AI-enabled CR-IoT user computes the updated means ($\bar{\mu}_{0,i,j}$, $\bar{\mu}_{1,i,j}$) based on line 8 and variances ($\bar{\sigma}^2_{0,i,j}$, $\bar{\sigma}^2_{1,i,j}$) based on line 9, respectively. Therefore, we concluded that the proposed enhanced KLD technique excludes the deep fading CR-IoT users.

Algorithm 1 The proposed enhanced KLD technique for an NU factor ($\rho > 1$) for an AI-enable CR-IoT network.

Input: $M_{\text{AI-CC}}, M_{\text{CC}}, N_s, f_s, T, \tau_s$, **and** τ_r

Output: $p_{f,\text{FC}}^{\overline{\text{KLD}}}$ **and** $p_{d,\text{FC}}^{\overline{\text{KLD}}}$

1: Initialize $N_s, M_{\text{AI-CC}}, M_{\text{CC}}$
2: **for** j from $M_{\text{AI-CC}}$ **do**
3: **for** i from M_{CC} **do**
4: **for** l from N_s **do**
5: Calculate: $e_{i,j} = \sum_{l=1}^{N_s} |y_{i,j}\left(\frac{l}{f_s}\right)|^2$
6: **end for**
7: Set: $e_{i,j} \sim \begin{cases} \aleph\left(\mu_{0,i,j}(H_0), \sigma^2_{0,i,j}(H_0)\right) \\ \aleph\left(\mu_{1,i,j}(H_1), \sigma^2_{1,i,j}(H_1)\right) \end{cases}$
8: Calculate: $\bar{\mu}_{0,i,j} = \frac{\sum_{i=1}^{M_{\text{CC}}} \mu_{0,i,j} - \mu_{0,i,j}}{(M_{\text{CC}}-1)}$ and $\bar{\mu}_{1,i,j} = \frac{\sum_{i=1}^{M_{\text{CC}}} \mu_{1,i,j} - \mu_{1,i}}{(M_{\text{CC}}-1)}$ with $\mu_{0,i,j}$ and $\mu_{1,i,j}$ in *(20)*
9: Calculate: $\bar{\sigma}^2_{0,i,j} = \frac{\sum_{i=1}^{M_{\text{CC}}} \sigma^2_{0,i,j} - \sigma^2_{0,i,j}}{(M_{\text{CC}}-1)}$ and $\bar{\sigma}^2_{1,i,j} = \frac{\sum_{i=1}^{M_{\text{CC}}} \sigma^2_{1,i,j} - \sigma^2_{1,i,j}}{(M_{\text{CC}}-1)}$ with $\sigma^2_{0,i,j}$ and $\sigma^2_{1,i,j}$ in *(21)*
10: Calculate: $\overline{\text{KLD}}(j) = \frac{1}{2}\left[\log\left(\frac{\bar{\sigma}^2_{0,i,j}}{\bar{\sigma}^2_{1,i,j}}\right) - 1 + \left(\frac{\bar{\sigma}^2_{1,i,j}}{\bar{\sigma}^2_{0,i,j}}\right) + \frac{\left(\bar{\mu}_{1,i,j} - \bar{\mu}_{0,i,j}\right)^2}{\bar{\sigma}^2_{0,i,j}}\right]$
11: **end for**
12: **if** $\sum_{j=1}^{M_{\text{NCC}}} \overline{\text{KLD}}(j) < \beta_{\text{KLD}}$ **then**
13: Set: $p_{f,\text{FC}}^{\overline{\text{KLD}}} = 1$
14: **else**
15: Set: $p_{f,\text{FC}}^{\overline{\text{KLD}}} = 0$
16: **end if**
17: **if** $\sum_{j=1}^{M_{\text{NCC}}} \overline{\text{KLD}}(j) \geq \beta_{\text{KLD}}$ **then**
18: Set: $p_{f,\text{FC}}^{\overline{\text{KLD}}} = 0$
19: **else**
20: Set: $p_{d,\text{FC}}^{\overline{\text{KLD}}} = 1$
21: **end if**
22: **end for**

The complexity given by the execution time of conventional ED and conventional KLD schemes are the same, which is defined by $\sum_{i=1}^{M} C_0 = C_0 \times M$, where C_0 is a constant that denotes the computing cost. Therefore, the Big O time complexity of the conventional ED and KLD schemes are $O(M)$. On the other hand, the execution time of the proposed enhanced KLD scheme is defined as $\sum_{i=1}^{M}\sum_{j=1}^{M_{AI-CC}} C_1 = C_1 \times M \times M_{AI-CC}$, where C_1 is a constant that denotes the computing cost of instructions from lines 1-22 of the proposed algorithm. Therefore, the Big O time complexity of the proposed enhanced KLD scheme based on Algorithm 1 is $O(M \times M_{AI-CC})$.

5. SIMULATION RESULTS AND DISCUSSION

The performance of the proposed enhanced KLD technique is evaluated through numerical simulations compared to other conventional techniques using the Monte Carlo method. The simulations have been executed using MATLAB, and the results are obtained from the average of 40 000–80 000 independent simulation runs. Moreover, the simulation parameters used are listed in Table 1.

Table 1 – Simulation parameters

Parameter	Value
Total number of CR-IoT users M_{CC}	4
Number of samples N_s	[20, 25, 30]
Total number of AI-CCs M_{AI-CC}	3
NU factor ρ	[1.00:.01:1.03]
Total number of CR-IoT users in a network M	15
Primary activity factors, P_0 & P_1	0.5
Sampling frequency f_s	300 KHz
Average SNR $\overline{\gamma}$	–6 dB
Sensing time slot τ_s	300 ms
Probability of the absence of the PU P_0	0.5
Reporting time slot for CR-IoT users, and AI-CCs τ_r	5 ms
Probability of the presence of the PU P_1	0.5
SNR at the PU link SNR_{PU}	10 dB
Energy consumption for the sensing duration E_s	1 J
SNR at the PU and CR-IoT link $SNR_{CR-IoT,i}$	7 dB
Energy consumption for the data transmission duration E_t	3 J
Global decision threshold β	3
Capacity of the battery E_c	300 J

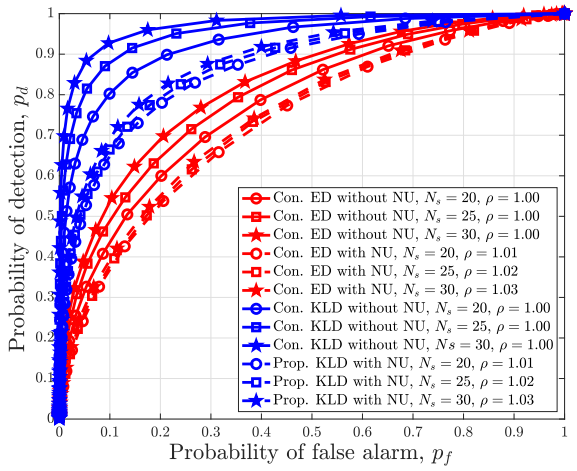

Figure 4 – The ROC curves for the proposed enhanced KLD technique and conventional ED and KLD techniques.

The sensing performance of the proposed enhanced KLD technique in comparison with the conventional ED technique, with and without NU, and conventional KLD without NU is plotted in Fig. 4 for $\overline{\gamma}_{i,j} = -4$ dB. First, it can be seen that all the techniques obtain greater sensing accuracy as the number of samples increases. Focusing on the proposed enhanced KLD technique with an NU factor $\rho > 1$, it can be seen that it achieves greater detection probability than all other conventional techniques except the conventional KLD technique assuming $\rho = 1$, i.e., without an NU factor. That is, the conventional ED technique suffers a degradation of the detection probability under NU. Furthermore, the proposed enhanced KLD technique with an NU factor $\rho > 1$ achieves lower detection probability in comparison with the conventional KLD technique in absence of NU, i.e., $\rho = 1$. As demonstrated in ***Theorem 2***, the proposed enhanced KLD technique cannot distinguish between non-deep fading and deep fading CR-IoT users because all CR-IoT users have the same or fixed SNR values, i.e., $\gamma_1 = \gamma_2 = \cdots = \gamma_{M_{CC}} = -4$ dB. Thus, notice that the harmful deep fading CR-IoT users participate in the CSS as normal CR-IoT users, which severely degrades the sensing performance.

The conventional KLD technique without an NU factor and the ED technique, with or without an NU factor, cannot exclude the deep fading CR-IoT users. As a consequence, their ROC curves degrade severely subject to NU. On the other hand, the proposed enhanced KLD technique with an NU factor is able to identify the deep fading CR-IoT users, and then, exclude them, which leads to a better sensing performance with increasing SNR values as shown in Fig. 5(a). Comparing the sensing gain at the FC, it can be seen that the proposed enhanced KLD technique can detect the primary spectrum with a detection probability of 86% compared to 69.5%, 57% and 97% obtained for the conventional ED technique without an NU factor, the conventional ED technique with an NU factor, and the conventional KLD technique without an NU factor, respectively, as listed in Table 2.

Table 2 – Sensing performance at the FC for an AI-enabled CR-IoT network for, $p_f = 0.2$ from Fig. 4.

Sensing performance p_d	$N_s = 20$	$N_s = 25$	$N_s = 30$
Conventional ED technique [$\rho = 1$]	0.600	0.645	0.695
Conventional ED technique [$\rho = 1.01, 1.02, 1.03$]	0.530	0.550	0.570
Conventional KLD technique [$\rho = 1$]	0.900	0.940	0.970
Proposed enhanced KLD technique [$\rho = 1.01, 1.02, 1.03$]	0.820	0.840	0.860

The ROC curves at the FC for the probability of detection and false alarm are shown in Fig. 5 for an SNR of the PU signal at the CR-IoT users from −13 dB to −3 dB under Rayleigh fading and shadowing conditions [27]. In Fig. 5(a), it can be seen that the sensing performance, as probability of detection, of the proposed enhanced KLD technique with an NU factor $\rho = 1.02$ considerably improves the performance of all other considered tech-

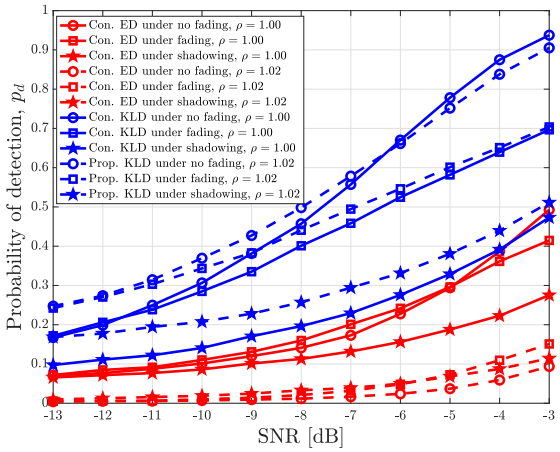

(a) Probability of detection, p_d.

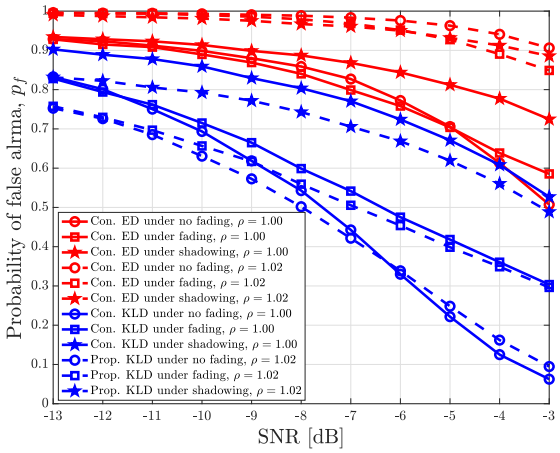

(b) Probability of false alarm, p_f.

Figure 5 – Probability of detection and probability of false alarm curves vs SNR at an FC centre of the proposed enhanced KLD technique in comparison with conventional ED and KLD techniques under a variety of the fading channels, where $N_s = 30$, $\rho = [1, 1.02]$) and $\gamma_{i,j} = [-13 : -3]$ dB.

niques. It is worth noticing that the NU factor, which is plotted for $\rho = 1$ and $\rho = 1.02$, on the ED technique drastically degrades the sensing performance. Even though an NU factor $\rho = 1.02$ can be considered large, the proposed enhanced KLD technique still achieves a better sensing performance. Therefore, we can conclude that the proposed enhanced KLD technique achieves a better sensing performance in comparison with the conventional techniques. Similarly, the false alarm of the proposed enhanced KLD technique with and without an NU factor $\rho = 1.02$ is lower when compared to other conventional techniques with an NU factor as is shown in Fig. 5(b).

The sum-rate for the conventional and proposed enhanced techniques depending on the probability of false alarm of a CR-IoT user is shown in Fig. 6. The sum-rate

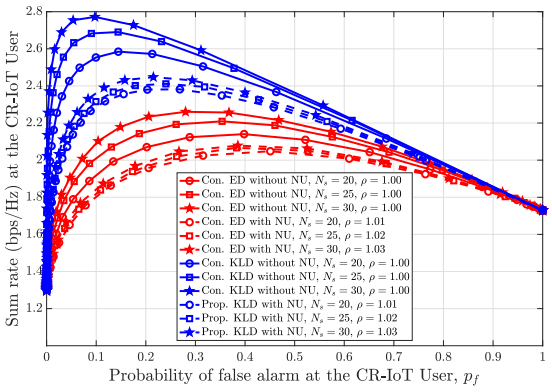

Figure 6 – Sum-rate vs probability of false alarm of CR-IoT user in the proposed enhanced KLD technique, and the conventional ED and KLD techniques when the number of samples $N_s = [20, 25, 30]$, an NU factor $\rho = [1, 1.01, 1.02, 1.03]$, and a primary activity factor $\alpha = 0.7$.

of the proposed enhanced technique outperforms all other conventional techniques in the entire range of the probability of false alarm. Furthermore, notice that the sum-rate curve is a quasi-concave function for the probability of false alarm. For $N_s = 30$ samples and $\rho = 1.03$ the sum-rate of the proposed enhanced KLD technique is equal to 2.49 bps/Hz, outperforming the conventional ED technique without an NU factor, the conventional ED technique with an NU factor and the conventional KLD technique without an NU factor that achieve 2.24 bps/Hz, 2.08 bps/Hz and 2.7 bps/Hz, respectively. It can be also seen that the conventional ED technique cannot realize an acceptable sensing performance with a small number of samples. To achieve a high probability of detection, firstly, the conventional ED technique requires a larger number of samples, i.e., a longer sensing period. Therefore, the proposed enhanced KLD technique realizes a higher probability of detection because the KLD technique performs well even with a small number of samples. It is worth noticing that short sensing intervals are essential in AI-enabled CR-IoT networks wherein a power saving operation is the most significant issue for a longer lifetime of the CR-IoT devices.

Until now, it has been shown that the proposed enhanced KLD technique achieves a greater sum-rate compared to the conventional ED techniques except the conventional KLD. This issue has been already discussed in the previous section in ***Theorem 1***. Thus, in order to validate ***Theorem 1*** through simulations, in Fig. 7(a). We plot the sum-rate for non-fixed SNR values for each CR-IoT in the following range $\gamma_{i,j} = [-13 : 1 : -3]$ dB. It can be seen that, under this assumption, the proposed enhanced KLD technique achieves a better sensing performance over the conventional KLD technique without an NU factor.

Fig. 7(b) shows the energy consumption for the proposed enhanced KLD technique with an NU factor $\rho = 1.02$ in comparison with the other considered techniques under

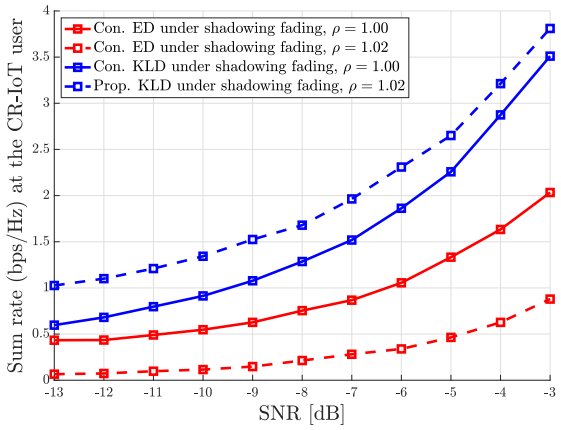

(a) Sum-rate of the CR-IoT users.

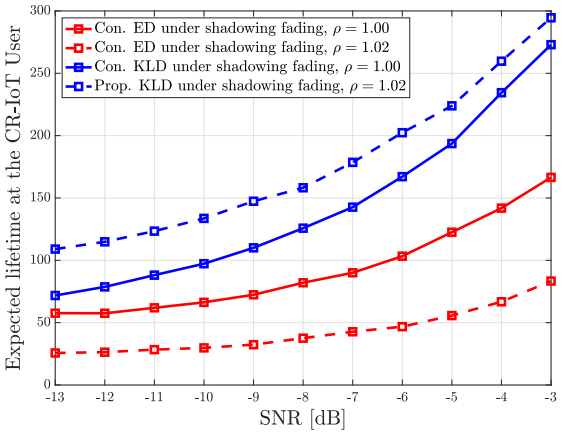

(a) Expected network lifetime. $E_s = 1$, $E_c = 300$, $E_t = 3$ $P_0 = P_1 = 0.5$

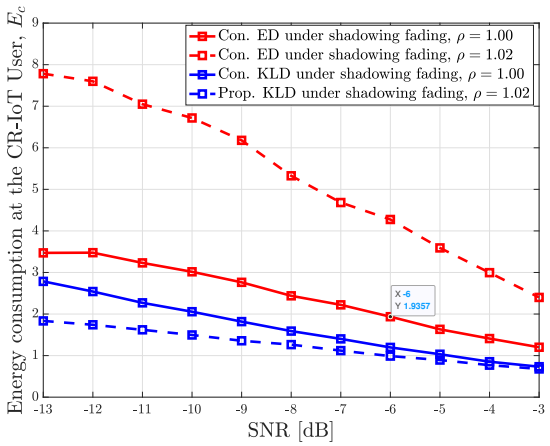

(b) Energy consumption of the CR-IoT users. $E_s = 1$, $E_t = 3$ $P_0 = P_1 = 0.5$

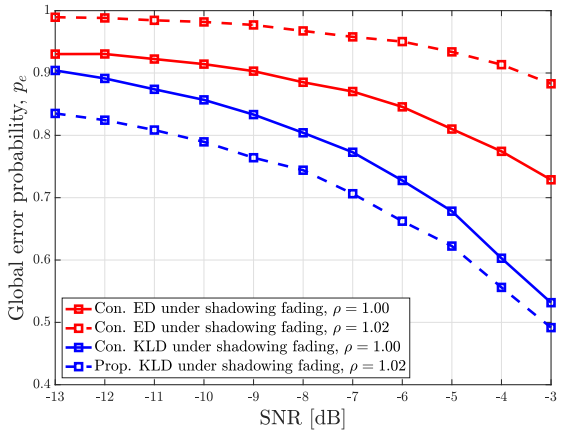

(b) Global error probability. $P_0 = P_1 = 0.5$

Figure 7 – Sum-rate curves and energy consumption vs SNR. Number of sample $N_s = 30$, $\gamma_{i,j} = [-13 : 1 : -3]$ dB and $\rho = [1, 1.02]$. Channel subject to the shadowing fading.

Figure 8 – Expected network lifetime and global error probability vs SNR. Number of sample $N_s = 30$, $\gamma_{i,j} = [-13 : 1 : -3]$ dB and $\rho = [1, 1.02]$. Channel subject to the shadowing fading.

shadow fading. Recall that the average energy consumption is a function of both the probability of detection and false alarm. It can be seen that the proposed KLD technique reduces considerably the energy consumption. Focusing on the SNR value $\gamma = -6$ dB, the proposed enhanced KLD technique consumes 1 J, while the conventional KLD technique without an NU factor, the conventional ED technique without a NU factor and the conventional ED technique with an NU factor consume 1.2 J, 1.85 J and 4.2 J, respectively.

The expected network lifetime of the proposed enhanced KLD technique with an NU factor $\rho = 1.02$ is shown in Fig. 8(a) compared to all the considered techniques. It can be seen that the proposed enhanced KLD technique outperforms the expected network lifetime for all other techniques. For an SNR equal to $\gamma = -6$ dB, it achieves an expected network lifetimes of about 200 rounds, while this value is below 165 for the KLD technique without an NU factor. Moreover, both conventional ED techniques, with and without an NU factor, are below 100 rounds. Therefore, the proposed enhanced KLD technique allows us to prolong the expected network lifetime compared with the other conventional techniques.

The global error probability of the proposed enhanced KLD technique and other conventional techniques with and without an NU factor is shown in Fig. 8(b). It can be seen that the proposed KLD technique with NU obtains the lowest global error probability. Moreover, note that the conventional ED technique with a NU factor obtains greater global error probability than the conventional ED technique without an NU factor. We can conclude that the proposed enhanced KLD technique with an NU factor allows us to reduce the global error probability.

6. CONCLUSION AND FUTURE WORK

In this work, we propose an enhanced KLD technique that makes use of an NU factor. The probability of detection, i.e., the sensing performance, of the proposed enhanced KLD technique outperforms the conventional techniques under no fading, fading and shadow fading channel conditions. Moreover, it provides an enhanced sum-rate compared to the conventional techniques. From an energy efficiency perspective, the proposed enhanced KLD technique with an NU factor obtains a lower energy consumption compared to conventional techniques. The network lifetime and the global error probability also improve for the proposed enhanced KLD technique. Further work will look at analyzing the sensing performance and sum-rate using the reporting framework while considering the interference to the PU link. In addition, a dynamic threshold of the proposed enhanced KLD technique will also be considered.

7. PROOF OF PROPOSITION 1

In an NU environment, the mean of the i^{th} CR-IoT user at the j^{th} AI-CC, $\mu_{1,i,j}$ under the hypothesis H_1 is given as

$$\begin{aligned}\mu_{1,i,j} &= \frac{N_s}{\rho}\left(|h_{i,j}|^2 p_x^2 + \sigma_{n,i,j}^2\right) = \frac{N_s}{\rho}\left(\left(1 + \frac{|h_{i,j}|^2 p_x^2}{\sigma_{n,i,j}^2}\right)\sigma_{n,i,j}^2\right) \\ &= \frac{N_s}{\rho}\left(1 + |h_{i,j}|^2\gamma_{i,j}\right)\sigma_{n,i,j}^2. \end{aligned} \tag{34}$$

Similarly, the variance of the i^{th} CR-IoT user at the j^{th} AI-CC, $\sigma_{1,i,j}^2$ under the hypothesis H_1 in an NU environment [28] is given as

$$\sigma_{1,i,j}^2 = \frac{N_s}{\rho}\left(E|x(l)|^4 + E|n_{i,j}(l)|^4 - (|h_{i,j}|^2 p_x^2 - \sigma_{n,i,j}^2)^2\right). \tag{35}$$

If the PU signal is a complex $\bar{M}$-ary Pulse Amplitude Modulation (M-PAM) signal [29], $E|x(l)|^4 = \left(3 - \frac{6}{5}\frac{\bar{M}^2+1}{\bar{M}^2-1}\right)|h_{i,j}|^4 p_x^4$. Thus, considering a BPSK modulated PU signal, we set $\bar{M} = 2$, and therefore, $E|x(l)|^4 = |h_{i,j}|^4 p_x^4$. Also, we consider the CSCG noise so that $E|n_{i,j}(l)|^4 = 2\sigma_{n,i,j}^4$. Finally, considering this definitions, we can rewrite *(35)* as

$$\begin{aligned}\sigma_{1,i,j}^2 =& \frac{N_s}{\rho}|h_{i,j}|^4 p_x^4 + 2\sigma_{n,i,j}^4 - \frac{N_s}{\rho}\left(|h_{i,j}|^4 p_x^4 - 2|h_{i,j}|^2 p_x^2 \sigma_{n,i,j}^2 + \sigma_{n,i,j}^4\right) \\ =& \frac{N_s}{\rho}\left(\sigma_{n,i,j}^4 + 2|h_{i,j}|^2 p_x^2 \sigma_{n,i,j}^2\right) = \frac{N_s}{\rho}\left(1 + 2|h_{i,j}|^2 \frac{p_x^2}{\sigma_{n,i,j}^2}\right)\sigma_{n,i,j}^4 \\ =& \frac{N_s}{\rho}\left(1 + 2|h_{i,j}|^2\gamma_i\right)\sigma_{n,i,j}^4. \end{aligned} \tag{36}$$

Now, substituting the value of the PU signal, $p_x^2 = 0$ in *(34)*, we can calculate the mean of the i^{th} CR-IoT user in j^{th} AI-CC, $\mu_{0,i,j}$ under hypothesis H_0 in a NU environment as $\mu_{0,i,j} = \rho N_s \sigma_{n,i,j}^2$. Also, substituting the value of the PU signal, $p_x^2 = 0$ in *(35)*, we can calculate the variance of the i^{th} CR-IoT user at the j^{th} AI-CC, $\sigma_{0,i,j}^2$ under the hypothesis H_0 in a NU environment as

$$\begin{aligned}\sigma_{0,i,j}^2 &= \rho N_s\left(E|n_{i,j}(l)|^4 - (\sigma_{n,i,j}^2)^2\right) \\ &= \rho N_s\left(2\sigma_{n,i,j}^4 - \sigma_{n,i,j}^4\right) = \rho N_s \sigma_{n,i,j}^4. \end{aligned} \tag{37}$$

8. PROOF OF PROPOSITION 2

Equation *(5)* can be rewritten as

$$\frac{\lambda_{i,j}^{\mathrm{ED}}}{\sqrt{\rho N_s}\sigma_{n,i,j}^2} = Q^{-1}\left(p_{f,j}\right) + \sqrt{\rho N_s}. \tag{38}$$

Thus, we can calculate the decision threshold, $\lambda_{i,j}^{\mathrm{ED}}$ at the i^{th} CR-IoT user of the j^{th} AI-CC using *(38)*,

$$\lambda_{i,j}^{\mathrm{ED}} = \sqrt{\rho N_s}\sigma_{n,i,j}^2 Q^{-1}\left(p_{f,j}\right) + \rho N_s \sigma_{n,i,j}^2. \tag{39}$$

Similarly, we can rewrite *(6)*) as

$$\frac{\lambda_{i,j}^{\mathrm{ED}}}{\sqrt{\frac{N_s}{\rho}}K\sigma_{n,i,j}^2} = Q^{-1}\left(p_{d,j}\right) + \frac{\sqrt{\frac{N_s}{\rho}}K^2}{K}. \tag{40}$$

Thus, we can calculate the decision threshold, $\lambda_{i,j}^{\mathrm{ED}}$ at the i^{th} CR-IoT user of the j^{th} AI-CC using the *(40)* as

$$\begin{aligned}\frac{\lambda_{i,j}^{\mathrm{ED}}}{\sqrt{\frac{N_s}{\rho}}K\sigma_{n,i,j}^2} &= \left(Q^{-1}\left(p_{d,j}\right) + \frac{\sqrt{\frac{N_s}{\rho}}K^2}{K}\right)\lambda_{i,j}^{\mathrm{ED}} \\ &= \sqrt{\frac{N_s}{\rho}}K\sigma_{n,i,j}^2\left(Q^{-1}\left(p_{d,j}\right) + \sqrt{\frac{N_s}{\rho}}K\right), \end{aligned} \tag{41}$$

where $K = \sqrt{(1 + 2|h_{i,j}|^2\gamma_{i,j})}$.

9. PROOF OF PROPOSITION 3

Putting the decision threshold, $\lambda_{i,j}^{\mathrm{ED}}$ value from *(39)* in *(41)*), and after some mathematical rearrangement, $N_s = \frac{\left[\sqrt{\rho}KQ^{-1}\left(p_{d,j}\right) - \rho^{\frac{3}{2}}Q^{-1}\left(p_{f,j}\right)\right]^2}{\left[\rho^2 - K^2\right]^2}$. Thus, the minimum number of samples can be expressed as in *(9)*.

$$\overline{\mathrm{KLD}}(j) = \frac{1}{2} \times \left[\log\left(\frac{\frac{\left(\sum_{i=1}^{M_{\mathrm{CC}}} \sigma_{0,i,j}^2 - \sigma_{0,i,j}^2\right)}{(M_{\mathrm{CC}}-1)}}{\frac{\left(\sum_{i=1}^{M_{\mathrm{CC}}} \sigma_{1,i,j}^2 - \sigma_{1,i,j}^2\right)}{(M_{\mathrm{CC}}-1)}} \right) - 1 + \left(\frac{\frac{\left(\sum_{i=1}^{M_{\mathrm{CC}}} \sigma_{1,i,j}^2 - \sigma_{1,i,j}^2\right)}{(M_{\mathrm{CC}}-1)}}{\frac{\left(\sum_{i=1}^{M_{\mathrm{CC}}} \sigma_{0,i,j}^2 - \sigma_{0,i,j}^2\right)}{(M_{\mathrm{CC}}-1)}} \right) + \frac{\left(\frac{\sum_{i=1}^{M_{\mathrm{CC}}} \mu_{1,i} - \mu_{1,i}}{M_{\mathrm{CC}}-1} - \frac{\sum_{i=1}^{M_{\mathrm{CC}}} \mu_{0,i} - \mu_{0,i}}{M_{\mathrm{CC}}-1} \right)^2}{\frac{\sum_{i=1}^{M_{\mathrm{CC}}} \sigma_{0,i,j}^2 - \sigma_{0,i,j}^2}{(M_{\mathrm{CC}}-1)}} \right] \tag{42}$$

$$\begin{aligned}
\overline{\mathrm{KLD}}(j) =& \frac{1}{2}\left(\log \frac{\sigma_{0,j}^2}{\sigma_{1,j}} \right) + \frac{1}{2}\left[\log\left(\frac{1 - \frac{\sigma_{0,i,j}^2}{M_{\mathrm{CC}}\sigma_{0,j}^2}}{1 - \frac{\sigma_{1,i,j}^2}{M_{\mathrm{CC}}\sigma_{1,j}^2}} \right) - 1 + \frac{1}{2}\left(\frac{M_{\mathrm{CC}}\sigma_{1,j}^2\left(1 - \frac{\sigma_{1,j,i}^2}{M_{\mathrm{CC}}\sigma_{1,j}^2}\right)}{\sigma_{0,j}^2\left(1 - \frac{\sigma_{0,j,i}^2}{\sigma_{0,j}^2}\right)} \right) \right] \\
&+ \frac{1}{2}\left[\frac{\left(M_{\mathrm{CC}}\mu_{1,j}\left(1 - \frac{\mu_{1,i,j}}{M_{\mathrm{CC}}\mu_{1,j}}\right) - M_{\mathrm{CC}}\mu_{0,j}\left(1 - \frac{\mu_{0,i,j}}{M_{\mathrm{CC}}\mu_{0,j}}\right)\right)^2}{(M_{\mathrm{CC}} - 1) \times M_{\mathrm{CC}}\sigma_{0,j}^2\left(1 - \frac{\sigma_{0,i,j}^2}{M_{\mathrm{CC}}\sigma_{0,j}^2}\right)} \right] \\
=& \frac{1}{2}\left[\log\left(\frac{\sigma_{0,j}^2}{\sigma_{1,j}} \right) \right] + \mathrm{KLD}(j)
\end{aligned} \tag{43}$$

10. PROOF OF THEOREM 1

From *(22)*, the following equation can be derived

$$\overline{\mathrm{KLD}}(j) = \frac{1}{2}\left[\log\left(\frac{\bar{\sigma}_{0,i,j}^2}{\bar{\sigma}_{1,i,j}^2} \right) - 1 + \left(\frac{\bar{\sigma}_{1,i,j}^2}{\bar{\sigma}_{0,i,j}^2} \right) + \frac{\left(\bar{\mu}_{1,i,j} - \bar{\mu}_{0,i,j}\right)^2}{\bar{\sigma}_{0,i,j}^2} \right]. \tag{44}$$

Based on the updated means and variance in *(20)* and *(21)*, we can rewrite *(44)* as shown in *(42)*. After some mathematical rearrangement, the expression *(43)* is obtained.

11. PROOF OF THEOREM 2

In a system subject to NU, the AI-CC cannot distinguish between the normal, i.e., non deep fading, CR-IoT users and users that suffer deep fading CR-IoT since the deep fading strength (X_μ, X_σ) is approximately the $\overline{\mathrm{KLD}}$ value under the hypothesis H_1 and H_0. As a result, the proposed enhanced KLD technique with an NU factor as not enhanced the sensing performance by the j^{th} AI-CC for deep fading CR-IoT users in an NU environment with an NU factor.

From *(22)*, we can rewrite it again as

$$\overline{\mathrm{KLD}}(j) = \frac{1}{2}\left[\log\left(\frac{\bar{\sigma}_{0,i,j}^2}{\bar{\sigma}_{1,i,j}^2} \right) - 1 + \left(\frac{\bar{\sigma}_{1,i,j}^2}{\bar{\sigma}_{0,i,j}^2} \right) + \frac{\left(\bar{\mu}_{1,i,j} - \bar{\mu}_{0,i,j}\right)^2}{\bar{\sigma}_{0,i,j}^2} \right]. \tag{45}$$

We can rewrite *(45)* based on the deep fading effect strength (X_μ, X_σ) as

$$\begin{aligned}
\overline{\mathrm{KLD}}(j) &= \frac{\overline{\mathrm{KLD}}(j)}{(X_\mu, X_\sigma)} \\
&= \frac{\overline{\mathrm{KLD}}(j)}{\left[X_\mu \xrightarrow{(H_0,H_1)} \left(\bar{\mu}_0 = \bar{\mu}_1\right), X_\sigma \xrightarrow{(H_0,H_1)} \left(\bar{\sigma}_0^2 = \bar{\sigma}_1^2\right) \right]} \\
&= \frac{1}{2}\left[\log\left(\frac{\bar{\sigma}_0^2}{\bar{\sigma}_0^2} \right) - 1 + \left(\frac{\bar{\sigma}_0^2}{\bar{\sigma}_0^2} \right) + \frac{\left(\bar{\mu}_0 - \bar{\mu}_0\right)^2}{\bar{\sigma}_0^2} \right] = 0,
\end{aligned} \tag{46}$$

where the i, j indexes have been omitted for the sake of clarity.

12. PROOF OF PROPOSITION 4

In an NU environment with an NU factor, we can calculate the total time required of the proposed enhanced KLD technique as

$$\begin{aligned}
\tau_t^{\overline{\mathrm{KLD}}} &= \tau_{dp} + \tau_s + \sum_{i=1}^{\frac{M}{M_{\mathrm{NCC}}}} \tau_{r,i} + \sum_{j=1}^{M_{\mathrm{NCC}}} \tau_{r,j} \\
&= \tau_{dp} + \tau_s + \left(\frac{M}{M_{\mathrm{NCC}}} \right)\tau_r + M_{\mathrm{NCC}}\tau_r \\
&= \tau_{dp} + \tau_s + \left(\frac{M}{M_{\mathrm{NCC}}} + M_{\mathrm{NCC}} \right)\tau_r \\
&= \tau_{dp} + \tau_s + \left(\frac{M + M_{\mathrm{NCC}}^2}{M_{\mathrm{NCC}}} \right)\tau_r.
\end{aligned} \tag{47}$$

ACKNOWLEDGMENT

This research was supported in part by the Machine Learning-aided Wireless Communications (MLWC) Research Laboratory, Deaprtment of Information and Communication Technology, Islamic University, Kushtia-7003, Bangladesh (Ref-No-141-EDU-IU-27-05-11-2024 & Ref-No-141-EDU-IU-2024-31-17-12-2024), in part by project IRENE-EARTH (PID2020-115323RBC33/AEI/10.13 039/ 501100011033), and in part by Bangladesh Bureau of Educational Information & Statistics (BANBEIS), Ministry of Education, Government of the People's Republic of Bangladesh (IC20201325).

REFERENCES

[1] Endong Tong, Wenjia Niu, Yunzhe Tian, Jiqiang Liu, Thar Baker, Sandeep Verma, and Zheli Liu. "A Hierarchical Energy-Efficient Service Selection Approach With QoS Constraints for Internet of Things". In: *IEEE Transactions on Green Communications and Networking* 5.2 (2021), pp. 645–657. DOI: 10.1109/TGCN.2021.3069121.

[2] Fatima Hussain, Syed Ali Hassan, Rasheed Hussain, and Ekram Hossain. "Machine Learning for Resource Management in Cellular and IoT Networks: Potentials, Current Solutions, and Open Challenges". In: *IEEE Communications Surveys Tutorials* 22.2 (2020), pp. 1251–1275. DOI: 10.1109/COMST.2020.2964534.

[3] Shakti Singh and Rahul Shrestha. "Ultra-Low Sensing-Time and Hardware-Efficient Spectrum Sensor for Data Fusion Based Cooperative Cognitive-Radio Network". In: *IEEE Transactions on Consumer Electronics* (2023).

[4] Danyang Wang, Peihan Qi, Qifan Fu, Ning Zhang, and Zan Li. "Multiple High-Order Cumulants-Based Spectrum Sensing in Full-Duplex-Enabled Cognitive IoT Networks". In: *IEEE Internet of Things Journal* 8.11 (2021), pp. 9330–9343.

[5] Md Sipon Miah, Heejung Yu, Tapan Kumar Godder, and Md Mahbubur Rahman. "A cluster-based cooperative spectrum sensing in cognitive radio network using eigenvalue detection technique with superposition approach". In: *International Journal of Distributed Sensor Networks* 11.7 (2015), p. 207935.

[6] Julio Manco and Iyad Dayoub. "Experimental assessment of spectrum sensing under time-varying channels for cognitive radio". In: *IEEE Sensors Letters* (2024).

[7] Mingyuan Dai, Jun Wu, Jifei Tang, Lanhua Xia, Jipeng Gan, Gefei Zhu, Jianrong Bao, and Weiwei Cao. "Energy-Efficient Quantized Data Fusion Based on Differential Mechanism in Cognitive Radio Networks". In: *IEEE Sensors Journal* (2024).

[8] Jungang Ge, Ying-Chang Liang, Shuo Wang, and Chen Sun. "RIS-Assisted Cooperative Spectrum Sensing for Cognitive Radio Networks". In: *IEEE Transactions on Wireless Communications* (2024).

[9] Muhammad Ejaz Ahmed, Dong In Kim, Jin Young Kim, and Yoan Shin. "Energy-arrival-aware detection threshold in wireless-powered cognitive radio networks". In: *IEEE Transactions on Vehicular Technology* 66.10 (2017), pp. 9201–9213.

[10] Shree Krishna Sharma, Tadilo Endeshaw Bogale, Symeon Chatzinotas, Björn Ottersten, Long Bao Le, and Xianbin Wang. "Cognitive radio techniques under practical imperfections: A survey". In: *IEEE Communications Surveys & Tutorials* 17.4 (2015), pp. 1858–1884.

[11] Morteza Tavana, Ali Rahmati, Vahid Shah-Mansouri, and Behrouz Maham. "Cooperative sensing with joint energy and correlation detection in cognitive radio networks". In: *IEEE Communications Letters* 21.1 (2016), pp. 132–135.

[12] Md Ruhul Amin, Md Mahbubur Rahman, Mohammad Amazad Hossain, Md Khairul Islam, Kazi Mowdud Ahmed, Bikash Chandra Singh, and Md Sipon Miah. "Unscented kalman filter based on spectrum sensing in a cognitive radio network using an adaptive fuzzy system". In: *Big Data and Cognitive Computing* 2.4 (2018), p. 39.

[13] Lucas dos Santos Costa, Dayan Adionel Guimarães, and Bartolomeu F Uchôa-Filho. "Influence of Noise Uncertainty Source and Model On the SNR Wall of Energy Detection". In: *IEEE Transactions on Cognitive Communications and Networking* (2024).

[14] Rahul Tandra and Anant Sahai. "SNR walls for signal detection". In: *IEEE Journal of selected topics in Signal Processing* 2.1 (2008), pp. 4–17.

[15] Yufan Chen, Lei Zhu, Yuchen Jiao, Changhua Yao, Kaixin Cheng, and Yuantao Gu. "An Extreme Value Theory-based Approach for Reliable Drone RF Signal Identification". In: *IEEE Transactions on Cognitive Communications and Networking* (2023).

[16] Md Miah, Kazi Mowdud Ahmed, Md Islam, Md Mahmud, Ashek Raihan, Md Rahman, Heejung Yu, et al. "Enhanced sensing and sum-rate analysis in a cognitive radio-based internet of things". In: *Sensors* 20.9 (2020), p. 2525.

[17] Noor Gul, Ijaz Mansoor Qureshi, Sadiq Akbar, Muhammad Kamran, and Imtiaz Rasool. "One-to-Many Relationship Based Kullback Leibler Divergence against Malicious Users in Cooperative Spectrum Sensing". In: *Wireless Communications and Mobile Computing* 2018 (2018).

[18] Natasha Zlobinsky, Amit K Mishra, and Albert A Lysko. "Spectrum Sensing and SINR Estimation in IEEE 802.11 s Cognitive Radio Ad Hoc Networks with Heterogeneous Interference". In: *IEEE Transactions on Wireless Communications* (2024).

[19] Tao Jiang, Ming Jin, Qinghua Guo, and Junteng Yao. "Graph learning-based cooperative spectrum sensing with corrupted RSSs in spectrum-heterogeneous cognitive radio networks". In: *IEEE Transactions on Wireless Communications* (2024).

[20] Ankit Mittal, Milin Zhang, Thomas Gourousis, Ziyue Zhang, Yunsi Fei, Marvin Onabajo, Francesco Restuccia, and Aatmesh Shrivastava. "Sub-6 GHz Energy Detection-Based Fast On-Chip Analog Spectrum Sensing with Learning-Driven Signal Classification". In: *IEEE Internet of Things Journal* (2024).

[21] Di He, Xin Chen, Ling Pei, Lingge Jiang, and Wenxian Yu. "Improvement of Noise Uncertainty and Signal-To-Noise Ratio Wall in Spectrum Sensing Based on Optimal Stochastic Resonance". In: *Sensors* 19.4 (2019), p. 841.

[22] Josip Lorincz, Ivana Ramljak, and Dinko Begušić. "A review of the noise uncertainty impact on energy detection with different OFDM system designs". In: *Computer Communications* (2019).

[23] Junlin Zhang, Lingjia Liu, Mingqian Liu, Yang Yi, Qinghai Yang, and Fengkui Gong. "MIMO spectrum sensing for cognitive radio-based Internet of things". In: *IEEE Internet of Things Journal* 7.9 (2020), pp. 8874–8885.

[24] MS Miah, M Schukat, and E Barrett. "Sensing and throughput analysis of a MU-MIMO based cognitive radio scheme for the Internet of Things". In: *Computer Communications* (2020).

[25] Sabyasachi Chatterjee, Prabir Banerjee, and Mita Nasipuri. "A new protocol for concurrently allocating licensed spectrum to underlay cognitive users". In: *Digital Communications and Networks* 4.3 (2018), pp. 200–208.

[26] Prabhat Thakur, Alok Kumar, S Pandit, G Singh, and SN Satashia. "Performance analysis of cognitive radio networks using channel-prediction-probabilities and improved frame structure". In: *Digital Communications and Networks* 4.4 (2018), pp. 287–295.

[27] Marvin K Simon and Mohamed-Slim Alouini. *Digital communication over fading channels*. Vol. 95. John Wiley & Sons, 2005.

[28] Stephen Boyd, Stephen P Boyd, and Lieven Vandenberghe. *Convex optimization*. Cambridge university press, 2004.

[29] Heinz Mathis. "On the kurtosis of digitally modulated signals with timing offsets". In: *2001 IEEE Third Workshop on Signal Processing Advances in Wireless Communications (SPAWC'01). Workshop Proceedings (Cat. No. 01EX471)*. IEEE. 2001, pp. 86–89.

AUTHORS

Md. Sipon Miah (Senior member, IEEE) was born in Gaibandha, Bangladesh, in January 1982. He received his B.Sc., M.Sc. and Ph.D. from the Department of Information and Communication Technology (ICT) at the Islamic University, Kushtia-7003, Bangladesh, in 2006, 2007, and 2016, respectively. He was a recipient of the three-year "ICT Ministry Scholarship" funded by the Ministry of ICT Division, Dhaka, Bangladesh, which he started in September 2013. In addition, he received his structured Ph.D. in computer science from the University of Galway, Galway, Ireland, in June 2021. During his structured Ph.D. programme (September 2016 – June 2021), he attended European doctoral schools organized by various European universities and organizations, and he successfully achieved all the credits leading him to obtain his structured Ph.D. degree with the European label. He was a recipient of the four-year structured Ph.D. "Hardiman Scholarship" funded by the University of Galway, Galway, Ireland, which he started in September 2016. Since 2010, he has been with the Department of Information and Communication Technology, Islamic University, Kushtia-7003, Bangladesh. He is currently a professor in the Department of ICT, Islamic University, Kushtia-7003, Bangladesh. He was a postdoctoral fellow in the Department of Signal Theory and Communications, University Carlos III of Madrid (UC3M), Leganes, Madrid, Spain. He was a recipient of the three-year research grant funded by University Carlos III of Madrid (UC3M) under the prestigious "30 Postdoctoral Fellowship", which he started in October 2021. Science October 2021, he has also been a research member of the Communications Group, in the department of Signal Theory and Communications, University Carlos III of Madrid (UC3M), Leganes, Madrid, Spain. He received the "Teaching Excellent Acknowledgment" Certificate for the course of Simulation and Optimization of Communication Systems from Vice-Rector of studies of UC3M. He was a visiting professor (short-term) in the Department of Energy and Electrical Engineering, Changan University, Xian, China. He received a "Best Presentation Award" from ICMEE-2023: 9th International Conference on Mechanical and Electronics Engineering in 2023. His research interests include cognitive radio-based Internet of Things, machine learning/deep learning-based wireless communications, THz communications, optimization-based wireless communications and massive MIMO antennas-based wireless communications. He is the editor of the book project entitled "AI-Driven Medical Imaging & Diagnosis" to be published by CRC Press, Taylor & Francis Group. The above research lines have produced more than 90 publications in international journals, presentations within international conferences, and book chapters with a total number of citations: 1400+, H-index: 16, i10-index: 27; reported by Google Scholar, Scopus, and ResearchGate. He serves as a member of the Editorial Board of Scientific Reports journal. He also acts as a referee in several highly reputed journals and international conferences.

Michael Schukat is a senior lecturer and researcher in the discipline of information technology at the University of Galway, Galway, Ireland. He is the principal investigator of both the Open Sensor Network Authentication (OSNA) cyber security research group (www.osna-solutions.com) and the Performance Engineering Laboratory @ NUI Galway. His main research interests include security/privacy problems of connected real-time /time-aware embedded systems (i.e., industrial control, IoT, and cyber-physical systems) and their communication/time synchronization protocols. He is actively involved in various security working groups on a European (e.g., COST Action Cryptacus) and International level (e.g., US-NIST CPS Public WG). Originally from Germany, Schukat studied computer science and medical Informatics at the University of Hildesheim, where he graduated with an M.Sc. (Dipl. Inf.) in 1994 and a Ph.D. (Dr. rer. nat.) in 2000. Between 1994 and 2002, he worked in various industry positions where he specialized in deeply embedded real-time systems across diverse domains, such as industrial control, medical devices, and automotive and network storage.

Enda Barrett is a lecturer and researcher at the University of Galway, Galway, Ireland. In 2013, Enda received his Ph.D. in computer science from University of Galway, Ireland. His Ph.D. research is an investigation about the application of a subset of machine learning techniques known as reinforcement learning to automate resource allocations and scale applications in infrastructure as a service cloud computing environments. Upon completion of his Ph.D., Enda joined Schneider Electric as a research engineer on a globally distributed innovation team. His main research interests include machine learning, distributed computing, cybersecurity and networking.

Maximo Morales Cespedes was born in Valdepeñas, Ciudad Real, Spain, in 1986. He received the B.Sc., M.Sc., and Ph.D. degrees from the Universidad Carlos III de Madrid, Spain, in 2010, 2012, and 2015, respectively, all in electrical engineering, with a specialization in multimedia and communications. In 2012, he was a finalist of the IEEE Region 8 Student Paper Contest. From 2015 to 2017, he was a postdoctoral fellow with the Institute of Information and Communication Technologies, Electronics and Applied Mathematics, Universite Catholique de Louvain. He is currently with the Department of Signal Theory and Communications, Universidad Carlos III de Madrid. His research interests include interference management, visible light communications, hardware implementations, MIMO techniques, and signal processing applied to wireless communications.

Ana Garcia Armada received a Ph.D. degree in electrical engineering from the Polytechnic University of Madrid in February 1998. She is currently a professor at Universidad Carlos III de Madrid, Spain. She is leading the Communications Research Group at this university. She has participated in more than 30 national and 10 international research projects, as well as having 20 contracts with the industry. Her research has resulted in nine book chapters, and more than 150 publications in prestigious international journals and conferences, as well as five patents. She has also contributed to standardization organizations (ITU, ETSI) and is a member of the European 5GPPP Group of Experts, as well as the Spanish representative on the committee of the ESA Joint Board on Communication Satellite Programs 5G Advisory Committee (5JAC). She has been the editor (2016–2019, Exemplary Editor Award 2017 and 2018) and area editor (2019-2020, Exemplary Editor Award 2020) of IEEE Communication Letters. She has been the editor of IEEE Transactions on Communications since 2019, area editor of IEEE Open Journal of the Communications Society since 2019, editor of the ITU Journal on Future and Evolving Technologies and is a regular member of the technical program committees of the most relevant international conferences in their field. She has formed / is part of the organizing committee of the IEEE Globecom 2019 and 2021 (General Chair), IEEE Vehicular Technology Conference Spring 2018, 2019 and Fall 2018, IEEE 5G Summit 2017, among others. She is Secretary of the IEEE ComSoc Signal Processing and Computing for Communications Committee, has been Secretary and Chair of the IEEE ComSoc Women in Communications Engineering Standing Committee. Since January 2020 she is Director of Online Content of the IEEE Communications Society. She has received the Award of Excellence from the Social Council and the Award for Best Teaching Practices from Universidad Carlos II de Madrid, as well as the third place Bell Labs Prize 2014, the Outstanding Service Award 2019 from the SPCE committee of the IEEE Communications Society and the Outstanding Service Award 2020 from the Women in Communications Engineering (WICE) standing committee.